Title

Characteristics of Focal Gamma Zone Parapapillary Atrophy

Journal

Investigative Ophthalmology & Visual Science, 61(3)

ISSN

0146-0404

Authors

Kim, Hae Rang
Weinreb, Robert N
Zangwill, Linda M
et al.

Publication Date

2020-03-16

DOI

10.1167/iovs.61.3.17

Peer reviewed

Characteristics of Focal Gamma Zone Parapapillary Atrophy

Hae Rang Kim,[1] Robert N. Weinreb,[2] Linda M. Zangwill,[2] and Min Hee Suh[1]

[1]Department of Ophthalmology, Haeundae Paik Hospital, Inje University College of Medicine, Busan, South Korea
[2]Hamilton Glaucoma Center, Shiley Eye Institute, and the Viterbi Family Department of Ophthalmology, University of California San Diego, La Jolla, California, United States

Correspondence: Min Hee Suh, Department of Ophthalmology, Haeundae Paik Hospital, Inje University College of Medicine, 1435 Jwa-dong, Haeundae-gu, Busan 612-030, Korea; crishuna6@gmail.com.

Received: June 2, 2019
Accepted: December 16, 2019
Published: March 16, 2020

Citation: Kim HR, Weinreb RN, Zangwill LM, Suh MH. Characteristics of focal gamma zone parapapillary atrophy. *Invest Ophthalmol Vis Sci.* 2020;61(3):17. https://doi.org/10.1167/iovs.61.3.17

Purpose. The purpose of this study was to investigate the characteristics of focal γ-zone parapapillary atrophy (focal γPPA) in patients with primary open-angle glaucoma (POAG) using spectral-domain optical coherence tomography (SD-OCT).

Methods. Three groups of POAG eyes ($n = 214$) were defined according to the circumferential extent of Bruch's membrane (BM) within the β-zone PPA, as follows: (1) no γPPA (intact BM; $n = 81$), (2) conventional γPPA (γPPA involving the fovea-BM-opening axis; $n = 89$), and (3) focal γPPA (γPPA not involving the fovea-BM-opening axis; $n = 44$). Clinical and ocular characteristics, including age, axial length (AXL), and focal lamina cribrosa (LC) defects were compared among the three groups.

Results. The focal γPPA group was significantly older (60.6 ± 11.0 years) and had shorter AXL (24.10 ± 1.34 mm) than those of the conventional γPPA group (46.2 ± 13.8 years and 26.53 ± 1.61 mm, respectively; $P < 0.001$). These values of the focal γPPA group were similar to those of the no γPPA group (23.73 ± 0.97 mm for AXL and 64.0 ± 13.0 years for age). The focal γPPA group had a significantly higher prevalence of focal LC defects than did the other two groups (70.5% [31/44] for the focal γPPA group versus 46.1% [41/89] for the conventional γPPA group versus 37.0% [30/81] for the no γPPA group; $P = 0.002$).

Conclusions. Focal γPPA was differentiated from conventional γPPA by older age and shorter AXL. Further, focal γPPA was frequently accompanied by focal LC defects. Longitudinal studies elucidating whether focal LC defects and focal γPPA share common pathogenesis are warranted.

Keywords: focal γ-zone parapapillary atrophy, focal lamina cribrosa defect, axial length

The β-zone parapapillary atrophy (βPPA) is characterized by the visibility of large choroidal vessels and sclera due to atrophy of the retinal pigment epithelium (RPE) and choriocapillaries adjacent to the optic nerve.[1,2] βPPA is correlated with both glaucoma severity and progression.[1,3,4] Moreover, recent reports have suggested that glaucoma progression and parapapillary deep-layer microvasculature differ according to PPA microstructure.[1,3,5–7] Glaucomatous eyes with PPA devoid of Bruch's membrane (BM; γPPA) were reported to be younger and more myopic than those manifesting βPPA with intact BM (βPPA_{+BM}).[8] Meanwhile, focal γPPA was newly recognized as an externally oblique border tissue (EOBT) localized to either the superior or inferior hemiretinae not involving the fovea-BM-opening axis.[5] In the same recent study, eyes with focal γPPA had relatively short axial length (AXL) relative to those with conventional γPPA.[5] These findings suggest that the characteristics of the deep optic nerve head (ONH) structures (i.e., lamina cribrosa [LC] and deep-layer microvasculature) of eyes with focal γPPA differ from those of eyes with conventional γPPA. However, little is known about this issue, despite its potential clinical importance for elucidation of the pathogenesis of glaucomatous ONH damage.

Therefore, the present study investigated the clinical features of patients with primary open-angle glaucoma (POAG) with focal γPPA in comparison with patients with conventional γPPA and those without γPPA.

Methods

This study enrolled patients with POAG who had visited the Haeundae Paik Hospital Glaucoma Clinic between January and November 2017. It was approved by the Institutional Review Board of Haeundae Paik Hospital. Informed consent was obtained from all of the subjects.[9]

Study Subjects

All of the participants underwent a complete ophthalmic examination, including visual acuity measurement, refraction tests, slit-lamp biomicroscopy, intraocular pressure (IOP) measurement by Goldmann applanation tonometry, gonioscopy, central corneal thickness (CCT) measurement with the Pentacam Scheimpflug imaging system (Oculus Optikgeräte GmbH, Germany), AXL measurement by IOL Master (Carl Zeiss Meditec, Dublin, CA, USA), dilated

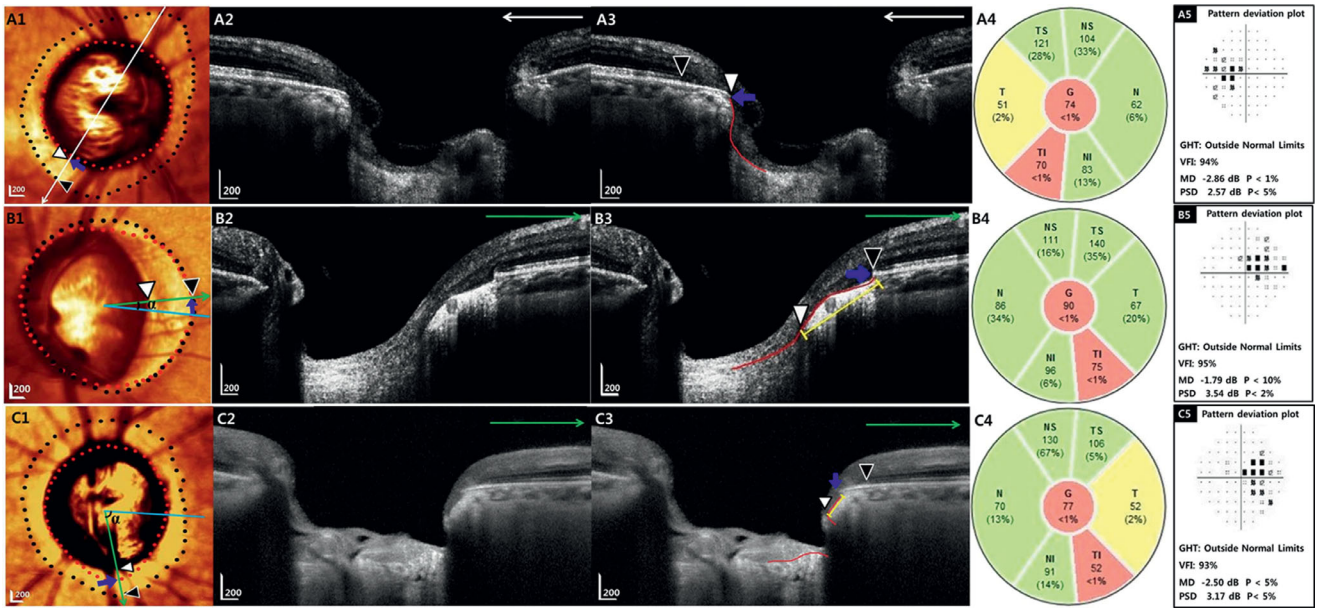

Figure 1. Representative cases of no γ-zone parapapillary atrophy (no γ PPA) group (**A**), conventional γPPA group (**B**), and focal γPPA group (**C**) showing differing age, axial length (AXL), and presence of focal lamina cribrosa (LC) defect. Color-converted infrared fundus images (**A1, B1, C1**) and spectral-domain optical coherence tomography (SD-OCT) images (**A2, A3**, **B2, B3, C2, C3**) with indications of retinal pigment epithelium (RPE) tip (black arrowheads, black dots), edge of Bruch's membrane (BM) (blue arrows, red dots), and optic disc margin (white arrowheads) are shown for each group (**A1-3, B1-3, C1-3**). White (**A1-3**) and green large arrows (**B1-3, C1-3**) indicate the location of the B-scans. **A**, Right eye of 67-year-old woman categorized as no γ PPA group had AXL of 23.31 mm. The BM was observed in the entire PPA region between the optic disc margin and RPE tip (**A1-3**). **B**, Left eye of 29-year-old man categorized as conventional γPPA group had AXL of 29.2 mm. The circumferential extent of the area without BM (blue arrows, red dots) was diffuse and involved the fovea-BM-opening axis (sky-blue line) (**B1-3**). The contours of the anterior laminar surface (red lines) of the no γ PPA group and conventional γPPA group were well preserved (**A2, A3, B2, B3**) **C**, Left eye of 57-year-old female categorized as focal γPPA group had AXL of 22.76 mm. The circumferential extent of the area without BM (blue arrows, red dots) was localized to the inferior hemi-retinae not involving the fovea-BM-opening axis (sky-blue line) (**C1-3**). Focal LC defect (red lines) was observed in the inferotemporal area, and its angular location was adjacent to that of the maximal external oblique border tissue (EOBT) (green arrow) (**C1-3**). The angular location of the maximal EOBT (yellow lines and green arrows; **B3, C3**) from the fovea-BM-opening axis was farther in an eye with focal γPPA (angle α; **C1**) than in an eye with conventional γPPA (angle α; **B1**). Note that focal γPPA group had significantly thinner RNFL in the TI sector (**C4**) than the other two groups (**A4, B4**) although the difference of visual field damage was not remarkable among the three eyes (**A5**, **B5**, **C5**).

fundus examination, simultaneous color and monochromatic fundus photography (TRC-NW8; Topcon, Tokyo, Japan), standard automated perimetry (Humphrey Field Analyzer; 30-2 Swedish Interactive Threshold Algorithm; Carl-Zeiss Meditec), and spectral-domain optical coherence tomography (SD-OCT). Presence of optic disc hemorrhage (DH) was defined as an isolated splinter- or flame-shaped hemorrhage on the ONH based on a standardized review of fundus photographs and/or regular optic disc examinations performed approximately every 3 to 6 months.[9] POAG was defined as the presence of an open angle with signs of glaucomatous optic nerve damage (i.e., the presence of focal thinning, notching, localized, or diffuse atrophy of the retinal nerve fiber layer [RNFL]) and ≥2 consecutive tests showing compatible glaucomatous visual field (VF) damage.[9]

Based on previous studies, only patients with POAG with visible βPPA on fundus photographs or optical coherence tomography (OCT) imaging and with a temporal width ≥100 µm on at least 1 radial scan measured by the built-in caliper of the SD-OCT as well as best-corrected visual acuity ≥20/40 were included in the current investigation.[3,5,7,10] Subjects with unreliable VFs or poor-quality OCT imaging, a history of ocular surgery (except for uncomplicated cataract or glaucoma surgery), non-glaucomatous intraocular diseases (e.g., diabetic retinopathy or non-glaucomatous optic neuropathy), or systemic diseases (e.g., stroke or pituitary tumor) that could influence the study results were excluded.[9] Those with systemic hypertension and diabetes mellitus were included unless they had been diagnosed with diabetic or hypertensive retinopathy.[5,10]

Spectralis Optical Coherence Tomography Imaging

The Spectralis SD-OCT2 Glaucoma Module Premium Edition (software version 1.7.0.0) was used to derive RNFL thickness and the PPA microstructure using a 9 × 9 mm-sized rectangular ONH Radial Circle (RC) scan centered on the ONH (Figs. 1A1-2, 1B1-2, 1C1-2). Details are available elsewhere.[9] Briefly, 24 consecutive radial equidistant B-scans subtending 15° starting from the fovea-BM-opening axis were acquired. Only high-quality images (quality score >15) were used in the analysis.[11] RNFL thickness was calculated at each point on a 3.5 mm-sized circle in a global area and in 6 sectors (superotemporal [TS], inferotemporal [TI], temporal [T], superonasal [NS], inferonasal [NI], and nasal [N]).

Analysis of β-zone Parapapillary Atrophy

The βPPA region defined as an area without RPE was evaluated around the temporal 180 degrees of the ONH using

the Spectralis software, which facilitated synchronous viewing of the color-converted infrared fundus images and the selected locations on the OCT B-scans.[5,9,12] The βPPA area was subdivided into βPPA_{+BM} defined as an area between the tips of the RPE and BM, and γPPA defined as an exposed border tissue between the clinical disc margin and the BM opening (Figs. 1A1-2, 1B1-2, 1C1-2).[3,5,7,8,12,13] Clinical disc margin was defined as an innermost clinically visible hyperreflective border on both the infrared fundus images and OCT. Both βPPA and γPPA were required to have a temporal width ≥100 µm on at least one radial OCT scan image, as measured by the built-in caliper of Spectralis OCT.[3,5,7,12]

According to the circumferential extent of the γPPA, the subjects were divided into three groups: (1) eyes without γPPA (no γPPA group) (Fig. 1A), (2) eyes with γPPA involving the fovea-BM-opening axis with minimum width at the fovea-BM-opening axis of ≥100 µm (conventional γPPA group; Fig. 1B), and (3) eyes with γPPA localized to either the superior or inferior hemi-retina with a width at the fovea-BM-opening axis of <100 µm (focal γPPA group; Fig. 1C).[5] These three PPA groups were determined independently by two experienced observers (H.R.K. and J.W.P.) masked to patients' clinical information.[5] Disagreements were resolved by consensus between the two observers. If consensus could not be reached, a third glaucoma specialist (M.H.S.) served as an adjudicator. If both eyes were included in the same group, one eye was randomly selected. If both eyes were eligible for different groups, they were assigned preferentially to the focal γPPA group, followed by the conventional γPPA, and no γPPA groups in consideration of prevalence.

The average of the βPPA and γPPA widths defined as the horizontal distances between the temporal optic disc boundary and the temporal margin of the RPE and BM tips, respectively, were calculated based on six radial scans of which the center was located at the fovea-BM-opening axis (Figs. 1A1-2, 1B1-2, 1C1-2).[9] If the temporal margin of the ONH or βPPA was not well visualized, adjacent radial scans 15° apart were used for the measurement. βPPA_{+BM} width was calculated as the difference between the βPPA and γPPA widths. In eyes with γPPA, the maximal γPPA width, the maximal EOBT length measured between the two end points of the EOBT, and their angular locations from the fovea-BM-opening axis were measured (Figs. 1B1-3, 1C1-3).[14] Positive and negative values of angular locations indicated locations that were superior or inferior to the fovea-BM-opening axis, respectively. The horizontal extent and angular location of each parameter were measured by two examiners (H.R.K. and J.W.P.) in a masked fashion using the built-in caliper tool of Spectralis SD-OCT. In addition, the horizontal and vertical widths of the clinical disc margin, defined as an innermost clinically visible hyper-reflective border both on the infrared fundus images and OCT, were measured by the two observers (H.R.K. and J.W.P.), respectively. The averages of the two examiners' measurements were used in the final analysis.

Focal Lamina Cribrosa Defect and Juxtapapillary Choroidal Thickness

Using a 20° × 20° high-resolution scan pattern that includes 48 radial B-scans in the enhanced depth imaging (EDI) mode, a focal LC defect was defined as laminar holes or laminar disinsertions violating the normal U- or W-shaped contour of the anterior laminar surface, as determined by two observers (M.H.S. and H.R.K.) in a masked fashion (Figs. 1A3, 1B3, 1C3).[15–17] Focal LC defects were required to be ≥100 µm in diameter and >30 µm in depth in at least 2 consecutive scans.[15–18] The subject was excluded from further analysis if consensus between the two observers could not be reached. The angular locations of the focal LC defects were determined with reference to the angle between the fovea-BM-opening axis and the center of focal LC defect. Positive and negative values of angular locations indicated locations that are superior or inferior to the fovea-BM-opening axis, respectively. If multiple focal LC defects were observed within the superior or inferior hemi-retinae simultaneously, the average angular location of each focal LC defect was derived.

The mean juxtapapillary choroidal thickness (JPCT) was calculated as the average of the JPCT measurements of two masked observers (H.R.K. and J.W.P.) at 24 meridians on 12 radial B-scan images of 20° × 20° EDI Spectralis SD-OCT using the built-in manual tool. The JPCT was defined as the choroidal area within 500 µm of the border tissue of the Elschnig.[19–21]

Data Analysis

The clinical characteristics, ONH morphological parameters, and focal LC defect were compared among the no γPPA, conventional γPPA, and focal γPPA groups. For comparing the continuous variables among the three groups, 1-way analysis of variance (ANOVA) and Tukey's test were performed for multiple comparisons and independent samples. To compare continuous variables of two groups, Student's *t*-test or Mann-Whitney *U* test was used depending on the normality. For categorical variables, χ^2 test with Bonferroni correction for multiple comparisons was performed. Bland-Altmann plots were used to compare the angular location of the maximal EOBT and focal LC defect, and to calculate interobserver agreements in measuring the horizontal and vertical widths of the clinical disc margin, and the horizontal extent and angular location of PPA, as well as the JPCT. Interobserver agreements in determining the three PPA groups and focal LC defects were assessed using the kappa coefficient. MedCalc (MedCalc, Inc., Mariakerke, Belgium) was used for the statistical analyses, and the α level (type I error) was set at 0.05.

Results

Baseline Characteristics of Study Subjects

Among 251 eyes of 251 consecutive patients with POAG, 37 were excluded for the following reasons: (1) poor-quality SD-OCT images that did not allow clear delineation of the choroid or determination of the βPPA microstructure (n = 16); (2) temporal βPPA or γPPA width <100 µm (n = 9); and (3) failure to reach consensus in determining the βPPA microstructure (n = 12). After the exclusions outlined above, 214 eyes of 214 patients (81 eyes of no γPPA group, 89 eyes of conventional γPPA group, and 44 eyes of focal γPPA group) were enrolled in this study.

Interobserver agreement was excellent for determination of the (1) three PPA groups and (2) presence of focal LC defects with Kappas (95% confidence interval [CI]) of 0.93 (0.88-0.97) and 0.87 (0.80-0.93), respectively; all P < 0.001. There were good interobserver reproducibility for measurement of JPCT (Bland-Altman 95% limit of agreement [LOA],

Table 1. Comparison of Baseline Characteristics Among the Three Groups of the PPA According to the Circumferential Extent of the PPA Without BM (γPPA)

Variables	Group 1 No γPPA	Group 2 Conventional γPPA	Group 3 Focal γPPA	*P* Value	Post Hoc
N	81	89	44		
Age, y	64.0 ± 13.0	46.2 ± 13.8	60.6 ± 11.0	**<0.001***	**2 < 1= 3**
Sex, M/F	42/39 (51.9%)	54/35 (60.7%)	20/24 (45.5%)	0.219†	
Spherical equivalent, D	−0.17 ± 1.87	−5.2 ± 3.9	−1.2 ± 2.8	**<0.001***	**1 = 3 < 2**
Axial length, mm	23.73 ± 0.97	26.53 ± 1.61	24.10 ± 1.34	**<0.001***	**1 = 3 < 2**
CCT, μm	538.9 ± 33.3	547.1 ± 40.3	539.1 ± 31.0	0.280*	
Baseline IOP, mm Hg	18.7 ± 7.0	17.2 ± 5.0	17.5 ± 6.5	0.282*	
IOP at examination, mm Hg	12.5 ± 2.7	12.3 ± 2.2	12.0 ± 2.9	0.534*	
Visual field MD, dB	−7.17 ± 6.58	−6.59 ± 5.14	−7.70 ± 6.22	0.578*	
Visual field PSD, dB	6.30 ± 3.59	7.43 ± 4.31	7.37 ± 4.37	0.154*	
RNFL thickness, μm					
Global area	73.5 ± 16.2	76.9 ± 16.7	72.9 ± 13.6	0.268*	
T	60.6 ± 14.9	63.4 ± 16.7	58.0 ± 15.0	0.157*	
TS	88.4 ± 34.6	85.1 ± 38.1	93.2 ± 35.0	0.475*	
NS	89.6 ± 30.6	86.2 ± 29.4	98.0 ± 29.4	0.104*	
N	65.1 ± 14.2	65.1 ± 23.5	67.5 ± 15.2	0.746*	
NI	83.2 ± 24.0	82.1 ± 27.4	79.3 ± 19.7	0.703*	
TI	85.8 ± 39.7	75.6 ± 33.3	70.7 ± 29.7	**0.046***	**3 < 1**
Disc hemorrhage, n (%)	9 (11.1)	13 (14.6)	7 (15.9)	0.703†	

Data are shown in mean ± SD.
* The comparison was performed by using 1-way analysis of variance with Tukey's correction.
† The comparison was performed by using Chi-squared test with Bonferroni correction.

Table 2. Comparison of the Optic Nerve Head Morphological Parameters, Presence of the Focal LC Defect, and JPCT Among the Three Groups of the PPA According to the Circumferential Extent of the PPA Without BM (γPPA)

Variables	Group 1 No γPPA	Group 2 Conventional γPPA	Group 3 Focal γPPA	*P* Value	Post Hoc
N	81	89	44		
BMO area, mm^2	2.1 ± 0.4	2.7 ± 0.8	2.4 ± 0.5	**<0.001***	**1 < 3 < 2**
Fovea-BMO angle, °	−7.6 ± 4.6	−7.0 ± 4.1	−8.2 ± 3.1	0.267*	
Average βPPA width, μm	232.8 ± 94.6	631.6 ± 232.9	279.8 ± 113.6	**<0.001***	**1 = 3 < 2**
Average βPPA_{+BM} width, μm	218.6 ± 84.0	217.2 ± 118.9	214.4 ± 110.2	0.977*	
Horizontal optic disc diameter, μm	1675.9 ± 154.3	1399.5 ± 302.1	1687.4 ± 192.3	**<0.001***	**2 < 1 = 3**
Vertical optic disc diameter, μm	1765.0 ± 185.0	1627.6 ± 310.9	1740.5 ± 187.4	**0.001***	**2 < 1 = 3**
JPCT, μm	119.8 ± 43.5	112.1 ± 33.7	121.3 ± 39.7	0.311*	
Focal LC defect, n (%)	30 (37.0)	41 (46.1)	31 (70.5)	**0.002‡**	**1 = 2 < 3**

Data are shown in mean ± SD.
* The comparison was performed by using 1-way analysis of variance with Tukey's correction.
‡ The comparison was performed by using Chi-squared test with Bonferroni correction.

−12.2 μm to 13.7 μm), average βPPA width (Bland-Altman 95% LOA, -33.7 μm to 27.2 μm), average βPPA_{+BM} width (Bland-Altman 95% LOA, -3.4 μm to 3.4 μm), maximal γPPA width (Bland-Altman 95% LOA, -76.9 μm to 65.9 μm), maximal EOBT length (Bland-Altman 95% LOA, -115.7 μm to 112.3 μm), angular location of maximal γPPA (Bland-Altman 95% LOA, -10.5° to 10.7°), maximal EOBT length (Bland-Altman 95% LOA, -11.8° to 14.4°), horizontal width of the clinical disc margin (Bland-Altman 95% LOA, -32.6 μm to 35.0 μm), vertical width of the clinical disc margin (Bland-Altman 95% LOA, -37.2 μm to 31.8 μm), and focal LC defect (Bland-Altman 95% LOA, -10.9° to 7.5°).

The demographics and clinical characteristics of the subjects are provided in Table 1. The three groups differed in age, spherical equivalent (SE), AXL, and RNFL thickness in the TI sector ($P < 0.05$). On post hoc analysis, the focal γPPA group was significantly older (60.6 ± 11.0 years), had shorter AXL (24.10 ± 1.34 mm), and a less myopic SE (-1.2 ± 2.8 D) relative to the conventional γPPA group (46.2 ± 13.8 years for age, 26.53 ± 1.61 mm for AXL, and -5.2 ± 3.9 D for SE, respectively; all $P < 0.001$), whereas the values in the focal γPPA group were similar to those of the no γPPA group (64.0 ± 13.0 years for age, 23.73 ± 0.97 mm for AXL, and -0.17 ± 1.87 D for SE; all $P > 0.10$). The focal γPPA group had significantly thinner RNFL in the TI sector (70.7 ± 29.7 μm) than the no γPPA groups (85.8 ± 39.7 μm; $P = 0.029$). None of the three groups differed in any of the other baseline characteristics, including sex, CCT, baseline IOP, IOP at examination, VF mean deviation (MD), VF pattern standard deviation (PSD), all RNFL thicknesses except that of the TI sector, and prevalence of DH (all $P > 0.10$; Table 1).

Comparison of ONH Morphological Parameters, Presence of Focal LC Defect, and JPCT Among Three Groups

Table 2 shows the data on the ONH morphological parameters and the presence of focal LC defect, and JPCT among

the three groups. The focal γPPA group had a significantly smaller BM-opening area (2.4 ± 0.5 mm^2), smaller βPPA (279.8 ± 113.6 μm), larger horizontal optic disc diameter (1687.4 ± 192.3 μm), and larger vertical optic disc diameter (1740.5 ± 187.4 μm) than did the conventional γPPA group (2.7 ± 0.8 mm^2 for BM-opening area, 631.6 ± 232.9 μm for βPPA width, 1399.5 ± 302.1 μm for horizontal optic disc diameter, and 1627.6 ± 310.9 μm for vertical optic disc diameter; all $P < 0.001$). The βPPA width and horizontal and vertical optic disc diameter of the focal γPPA group were similar to those of the no γPPA group (232.8 ± 94.6 μm for βPPA width, 1675.9 ± 154.3 μm for horizontal optic disc diameter, and 1765.0 ± 185.0 μm for vertical optic disc margin), and BM-opening area (2.4 ± 0.5 mm^2) of focal γPPA group was significantly larger than that of no γPPA group (2.1 ± 0.4 mm^2; $P < 0.001$). The prevalence of focal LC defects was significantly higher in the focal γPPA group than in the other two groups (70.5% [31/44] in the focal γPPA group, 37.0% [30/81] in the no γPPA group, and 46.1% [41/89] in the conventional γPPA group, respectively; $P = 0.002$). The three groups did not differ in fovea-BM-opening angle, βPPA_{+BM} width or JPCT (all $P > 0.10$).

Comparison of the Parameters of VF and RNFL Thickness According to the Presence of LC Defects Among Three Groups

Parameters of VF and RNFL were compared between eyes with and without focal LC defect in each of the three γPPA groups (Table 3). Eyes with a focal LC defect had a significantly thinner RNFL in the TI sector in all three γPPA groups ($P < 0.05$). Meanwhile, RNFL thicknesses of all other areas and all VF parameters did not differ according to the presence of focal LC defect in all three γPPA groups ($P > 0.05$), except the TS sector of focal γPPA group, in which eyes with focal LC defect had thicker RNFL than those without focal LC defect ($P = 0.039$).

Comparison of Characteristics of γPPA Between Eyes With Focal γPPA and Conventional γPPA

The characteristics of γPPA comparing the focal γPPA and conventional γPPA groups are shown in Table 4. The focal γPPA group had a significantly shorter maximal γPPA width (181.5 ± 82.9 mm), a shorter maximal EOBT length (229.5 ± 79.1 mm), as well as a maximal γPPA (-45.0 ± 47.7°), and a maximal EOBT (-46.3 ± 49.1°) located away from the fovea-BM-opening axis relative to the conventional γPPA group (524.8 ± 221.2 mm for maximal γPPA width, 576.9 ± 221.2 mm for maximal EOBT length, −15.7 ± 24.6° for maximal γPPA angular location, and -14.9 ± 26.2° for maximal EOBT angular location; all $P < 0.001$).

Topographic Relationship Between γPPA and Focal LC Defect in Eyes With γPPA

Figure 2 characterizes the relationship between the angular location of maximal EOBT and that of focal LC defect in the focal γPPA and conventional γPPA groups. There was closer topographical agreement between the locations of maximal EOBT and focal LC defect in the focal γPPA group (Bland-Altman 95% LOA, -30.7° to 33.8°; Fig. 2A) than in the conventional γPPA group (Bland-Altman 95% LOA, -45.1° to 109.5°; Fig. 2B).

Discussion

Focal γPPA with exposed scleral flange localized to the inferior or superior hemi-retinae has recently been described, and eyes with focal γPPA had relatively short AXL.[5] The present study extends the characterization of focal γPPA and suggests that in addition to a shorter AXL, these eyes have a smaller BM-opening area, and smaller βPPA relative to those with conventional γPPA. Most importantly, the focal γPPA group showed a higher prevalence of focal LC defects than did the conventional γPPA and no γPPA groups; and better spatial correlation between the focal LC defect and maximal EOBT than in the conventional γPPA group. These findings suggest that development of focal LC defect and that of focal γPPA might share a common pathogenesis.

Recently, Lee et al. suggested that development of γPPA and a focal LC defect during axial elongation are mainly caused by nasal shifting of the LC and vulnerability on the opposite side of the LC shift from subsequent scleral expansion and LC damage.[22–24] Further, their recent study showed that eyes with a mild shift of the LC had larger angular deviation of vascular trunk against the horizontal midline and a higher prevalence of a focal LC defect than did those with moderate or severe shift.[23] These findings correspond well with the current results showing that eyes with focal γPPA had a higher prevalence of a focal LC defect and a maximal EOBT located farther from the fovea-BM-opening axis than did eyes with conventional γPPA.[23] When the axis of LC shift is highly deviated from the horizontal axis, it collides easily with the radially oriented collagen fiber of the scleral tissue,[23,25] and, as such, might lead to high susceptibility to focal LC damage and concurrent development of focally extended scleral flange. On the other hand, it is also possible that mechanisms other than axial elongation play a role in the development of focal γPPA.[5] The present focal γPPA group was older and had a shorter AXL than the conventional γPPA group, and their age and AXL were comparable to those of the no γPPA group. Therefore, the development of small exposed border tissue in aged patients with relatively short AXL might not be fully explained by an LC shift incurred by axial elongation. In these circumstances, morphological LC change incurred by sustained vertical force related to IOP could serve as a potential mechanism of adjacent-border-tissue dragging. This process, moreover, might be facilitated by altered biomechanical properties of the LC and border tissue as well as by increased IOP. In this respect, the current observations that focal γPPA group had thinner RNFL than no γPPA group in the TI sector, an area in which focal LC defect and maximal focal γPPA frequently develop add to the literature.[14] Because focal LC defects are known to be closely associated with functional and structural damage to RGC axons,[11,26,27] development of an EOBT, glaucomatous RNFL defect, and focal LC defect may share a common pathway. Similarly, eyes with a focal LC defect had significantly thinner RNFL in the TI sector in all three subgroups of γPPA. However, the present study is limited in such speculations due to its cross-sectional nature and lack of differences in the VF parameters according to the presence of focal γPPA and focal LC defect. Lack of the VF differences may be because the disease severity of the current study population was relatively mild (average VF MD, -7.08 dB) compared with that of a previous study (average VF MD, -11.64 dB), which showed the relationship between the focal LC defect and VF severity.[27] Another recent study on eyes having early to moderate glaucoma (average VF MD,

Table 3. Comparison of the Parameters of Visual Field and RNFL Thickness According to the Presence of LC Defects Among the Three PPA Groups According to the Circumferential Extent of the PPA Without BM (γPPA)

	Group 1 No γPPA ($n = 81$)			Group 2 Conventional γPPA ($n = 89$)			Group 3 Focal γPPA ($n = 44$)		
	Focal LC Defect (+)	Focal LC Defect (−)	*P* Value*	Focal LC Defect (+)	Focal LC Defect (−)	*P* Value*	Focal LC Defect (+)	Focal LC Defect (−)	*P* Value*
N	30	51		41	48		31	13	
Visual field MD, dB	−8.2 ± 7.3	−6.5 ± 6.0	0.260	−7.5 ± 5.3	−5.9 ± 5.0	0.135	−8.3 ± 6.6	−7.2 ± 6.3	0.592
Visual field PSD, dB	6.9 ± 3.7	6.0 ± 3.6	0.236	8.5 ± 4.3	6.7 ± 4.2	0.052	8.1 ± 4.2	6.4 ± 4.5	0.220
Superior retinal	18.4 ± 7.3	21.3 ± 7.4	0.090	19.8 ± 7.9	22.1 ± 7.5	0.160	19.1 ± 8.7	22.3 ± 7.2	0.243
Inferior retinal	22.8 ± 7.8	23.1 ± 6.2	0.857	25.0 ± 6.3	25.7 ± 4.5	0.499	23.9 ± 6.6	22.5 ± 7.4	0.552
Superior TD	−10.2 ± 7.5	−7.7 ± 7.8	0.164	−10.1 ± 8.3	−7.7 ± 7.8	0.176	−9.8 ± 8.9	−6.7 ± 7.3	0.279
Inferior TD	−7.2 ± 8.0	−6.9 ± 6.1	0.844	−6.0 ± 6.2	−5.2 ± 4.4	0.498	−6.3 ± 6.8	−8.6 ± 9.6	0.368
RNFL thickness, µm									
Global area	71.0 ± 13.6	75.2 ± 17.4	0.266	74.8 ± 17.2	78.5 ± 16.5	0.311	73.0 ± 13.9	71.3 ± 15.0	0.719
T	58.5 ± 12.4	62.3 ± 15.7	0.263	60.0 ± 15.3	66.2 ± 16.8	0.080	58.1 ± 14.6	56.6 ± 16.9	0.765
TS	94.4 ± 36.0	85.7 ± 32.8	0.270	83.1 ± 40.1	86.6 ± 37.2	0.671	99.0 ± 34.6	75.1 ± 32.7	**0.039**
NS	90.6 ± 36.0	88.6 ± 27.6	0.779	82.8 ± 27.0	88.7 ± 31.2	0.362	101.4 ± 30.8	85.8 ± 25.4	0.116
N	65.0 ± 12.0	64.9 ± 15.7	0.986	62.5 ± 21.9	67.4 ± 24.6	0.340	68.4 ± 15.8	64.7 ± 13.5	0.462
NI	78.5 ± 23.5	86.3 ± 23.5	0.155	80.3 ± 21.7	83.6 ± 31.2	0.585	78.9 ± 20.8	78.3 ± 19.5	0.926
TI	66.6 ± 27.9	98.0 ± 40.7	**<0.001**	65.9 ± 31.3	82.1 ± 33.5	**0.024**	61.0 ± 23.5	96.0 ± 33.4	**<0.001**

* The comparison was performed by using 1-way analysis of variance with Tukey's correction.

Table 4. Comparison of the Characteristics of Parapapillary Atrophy Without BM (γPPA) Between Eyes with Focal γPPA and Conventional γPPA

Variables	Conventional γPPA	Focal γPPA	*P* Value*
N	89	44	
Horizontal extent			
Maximal γPPA width, μm	524.8 ± 221.2	181.5 ± 82.9	**<0.001**
Maximal EOBT length, μm	576.9 ± 221.2	229.5 ± 79.1	**<0.001**
Angular location			
Maximal γPPA location, °	−15.7 ± 24.6	−45.0 ± 47.7	**<0.001**
Maximal EOBT location, °	−14.9 ± 26.2	−46.3 ± 49.1	**<0.001**

* The comparison was performed by using Mann Whitney test.

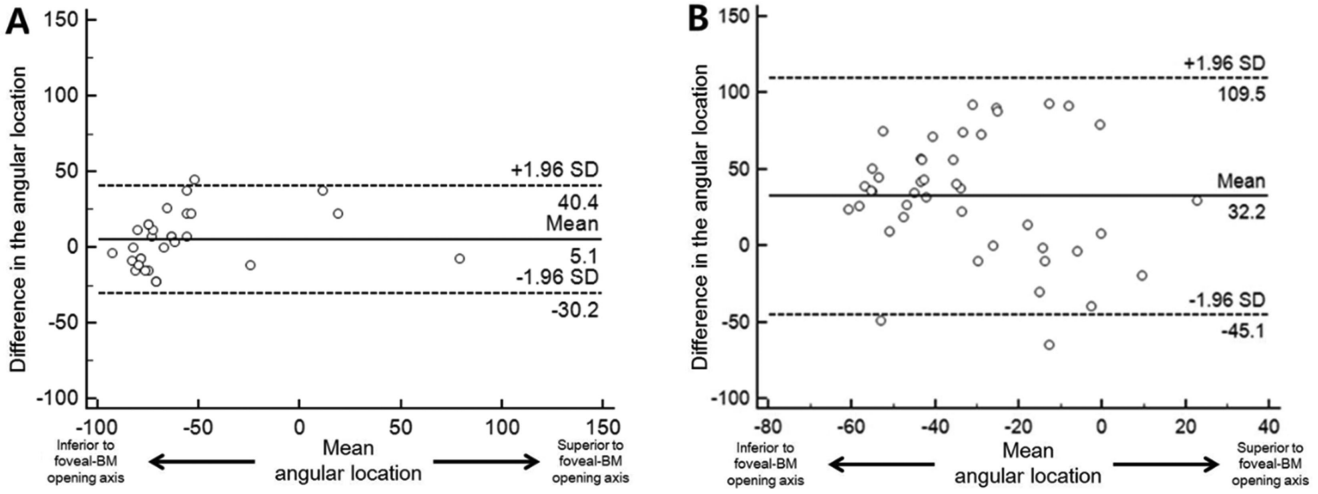

Figure 2. Bland-Altman plots showing relationship between angular location of maximal external oblique border tissue (EOBT) and that of focal lamina cribrosa (LC) defect in eyes with γ-zone parapapillary atrophy without Bruch's membrane (BM) not involving the fovea-BM-opening axis (focal γPPA) ($n = 44$) (**A**), and in eyes with γPPA involving the fovea-BM-opening axis (conventional γPPA) ($n = 89$) (**B**). The solid lines show the mean difference, and the dashed lines represent the 95% limit of agreement (LOA). The positive and negative values represent the locations of maximal EOBT and focal LC defect that are superior and inferior to the fovea-BM-opening axis, respectively.

−4.19 dB) showed that VF severity did not differ according to the presence of a LC defect.[28] Further, longitudinal studies on patients with glaucoma with various disease severities are warranted to elucidate the causal relationships among axial elongation, morphological change of LC, and border tissue, as well as glaucomatous VF and RNFL damage.

In this regard, comparison of the PPA microstructure of glaucomatous eyes with that of the normal healthy subjects is needed to prove the pathogenic role of the focal γPPA in the development of glaucomatous optic neuropathy and focal LC defect. In our pilot study on 47 healthy normal eyes with ßPPA, only 6.4% (3/47) had focal γPPA and none had focal LC defect, whereas 42.6% (20/47) and 51.1% (24/47) were categorized as conventional γPPA and no γPPA group, respectively (data not shown). This suggests that focal γPPA may be closely associated with the pathogenesis of glaucomatous optic neuropathy. Further studies comparing the prevalence of focal γPPA between the glaucoma and healthy normal eyes are needed.

In the present study, JPCT did not differ among the three groups (all $P > 0.10$). This result is consistent with a previous study that found that neither AXL nor γPPA width were associated with JPCT.[19] Given that the relationship of choroidal thickness with axial elongation and PPA width is controversial,[19,29–32] future studies concerning the influence of the PPA microstructure on the choroidal structure are warranted.

It has been reported that small disc size and long AXL might be related to the development of the focal LC defect.[33,34] In this study, the focal γPPA group had a significantly larger width of both the horizontal and vertical optic disc widths and shorter AXL than the conventional γPPA group. Moreover, the values in the focal γPPA group were similar to those in the no γPPA group (Table 2). These findings suggest that the influence of optic disc size and AXL on the detection of focal LC defect is not remarkable.

There are several limitations to this study. First, as noted above, the present study was cross-sectional and did not assess the location of vascular trunk and VF/RNFL damage. Second, focal γPPA was defined arbitrarily as an exposed scleral flange measured at the fovea-BM-opening axis to <100 μm. This was based on the observations of our recent study that all eyes with focal γPPA had an exposed scleral flange with a width <100 μm as measured at the fovea-BM-opening axis.[5] In the present study, conventional γPPA mainly incurred by axial elongation that led to temporal dragging of the ONH around the central horizontal fovea–BM-opening axis, had a width of exposed scleral flange >100 μm.[5,8] Third, only the temporal 180 degrees of the PPA was analyzed in this study, due to poor-quality SD-OCT images of the nasal area in some eyes. Therefore, a few eyes with βPPA or γPPA located mainly in the nasal area ($n = 7$) were excluded from the analysis. Further

improvement of SD-OCT images should enable detailed investigation of the clinical implications of eyes with βPPA or γPPA located in the nasal area. Finally, because this study's sample size is relatively small due to exclusion of relative large number of subjects (37 of 251 eyes) and it is a hospital-based study, differences between the three groups may not be representative of differences in the characteristics of γPPA in a general population of patients with glaucoma.

In conclusion, eyes with focal γPPA localized to the superior or inferior hemi-retinae were of older age and had shorter AXL and smaller βPPA relative to those with conventional γPPA. Furthermore, the focal γPPA group showed a higher prevalence of focal LC defect than did the conventional γPPA and no γPPA groups. These findings suggest that focal γPPA and focal LC defect share a common pathogenic mechanism in glaucomatous optic nerve damage.

Acknowledgments

The authors thank Jun Woo Park, MD, and Ji Min Kwon, MD, for their data acquisition.

Supported in part by National Eye Institute (R01EY029058) and an unrestricted grant by Research to Prevent Blindness (New York, NY [LMZ]). The authors alone are responsible for the content and writing of the paper.

Disclosure: **H.R. Kim,** None; **R.N. Weinreb,** Allergan (C), Bausch & Lomb (C), Carl Zeiss Meditec (F), Eyenovia (C), Genentech (F), Heidelberg Engineering (F), National Eye Institute (F), Novartis (C), Optos (F), Optovue (F), Unity (C); **L.M. Zangwill,** Carl Zeiss Meditec (F), Heidelberg Engineering (F), Merck (C), National Eye Institute (F), Optovue (F), Topcon (F); **M.H. Suh**, None

References

1. Teng CC, De Moraes CGV, Prata TS, Tello C, Ritch R, Liebmann JM. β-Zone parapapillary atrophy and the velocity of glaucoma progression. *Ophthalmology*. 2010;117:909–915.
2. Jonas JB, Nguyen XN, Gusek GC, Naumann GOH. Parapapillary chorioretinal atrophy in normal and glaucoma eyes. I. Morphometric data. *Investig Ophthalmol Vis Sci*. 1989;30:908–918.
3. Kim YW, Lee EJ, Kim TW, Kim M, Kim H. Microstructure of β-zone parapapillary atrophy and rate of retinal nerve fiber layer thinning in primary open-angle glaucoma. *Ophthalmology*. 2014;121:1341–1349.
4. Uchida H, Ugurlu S, Caprioli J. Increasing peripapillary atrophy is associated with progressive glaucoma. *Ophthalmology*. 1998;105:1541–1545.
5. Suh MH, Zangwill LM, Manalastas PIC, et al. Deep-layer microvasculature dropout by optical coherence tomography angiography and microstructure of parapapillary atrophy. *Investig Ophthalmol Vis Sci*. 2018;59:1996–2004.
6. Lee EJ, Kim TW, Kim JA, Kim JA. Parapapillary deep-layer microvasculature dropout in primary open-angle glaucoma eyes with a parapapillary gamma-zone. *Invest Ophthalmol Vis Sci*. 2017;58:5673–5680.
7. Lee SH, Lee EJ, Kim TW. Topographic correlation between juxtapapillary choroidal thickness and parapapillary deep-layer microvasculature dropout in primary open-angle glaucoma. *Br J Ophthalmol*. 2018;102:1134–1140.
8. Kim M, Kim TW, Weinreb RN, Lee EJ. Differentiation of parapapillary atrophy using spectral-domain optical coherence tomography. *Ophthalmology*. 2013;120:1790–1797.
9. Suh MH, Park JW, Kim HR. Association between the deep-layer microvasculature dropout and the visual field damage in glaucoma. *J Glaucoma*. 2018;27:543–551.
10. Suh MH, Zangwill LM, Manalastas PIC, et al. Deep retinal layer microvasculature dropout detected by the optical coherence tomography angiography in glaucoma. *Ophthalmology*. 2016;123:2509–2518.
11. Tatham AJ, Miki A, Weinreb RN, Zangwill LM, Medeiros FA. Defects of the lamina cribrosa in eyes with localized retinal nerve fiber layer loss. *Ophthalmology*. 2014;121:110–118.
12. Park JW, Suh MH, Agrawal R, Khandelwal N. Peripapillary choroidal vascularity index in glaucoma—A comparison between spectral-domain OCT and OCT angiography. *Investig Opthalmology Vis Sci*. 2018;59:3694.
13. Suh MH, Park JW, Khandelwal N, Agrawal R. Peripapillary choroidal vascularity index and microstructure of parapapillary atrophy. *Invest Ophthalmol Vis Sci*. 2019;60:3768–3775.
14. Han JC, Lee EJ, Kim SB, Kee C. The characteristics of deep optic nerve head morphology in myopic normal tension glaucoma. *Investig Ophthalmol Vis Sci*. 2017;58:2695–2704.
15. Suh MH, Zangwill LM, Manalastas PIC, et al. Optical coherence tomography angiography vessel density in glaucomatous eyes with focal lamina cribrosa defects. *Ophthalmology*. 2016;123:2309–2317.
16. You JY, Park SC, Su D, Teng CC, Liebmann JM, Ritch R. Focal lamina cribrosa defects associated with glaucomatous rim thinning and acquired pits. *JAMA Ophthalmol*. 2013;131:314–320.
17. Kiumehr S, Park SC, Syril D, et al. In vivo evaluation of focal lamina cribrosa defects in glaucoma. *Arch Ophthalmol (Chicago, Ill 1960)*. 2012;130:552–559.
18. Kim YK, Park KH. Lamina cribrosa defects in eyes with glaucomatous disc haemorrhage. *Acta Ophthalmol*. 2016;94:e468–e473.
19. Lee SH, Lee EJ, Kim TW. Topographic correlation between juxtapapillary choroidal thickness and microstructure of parapapillary atrophy. *Ophthalmology*. 2016;123:1965–1973.
20. Lee KM, Lee EJ, Kim TW. Juxtapapillary choroid is thinner in normal-tension glaucoma than in healthy eyes. *Acta Ophthalmol*. 2016;94:e697–e708.
21. Lee EJ, Kim TW, Lee SH, Kim JA. Underlying microstructure of parapapillary deep-layer capillary dropout identified by optical coherence tomography angiography. *Investig Ophthalmol Vis Sci*. 2017;58:1621–1627.
22. Lee KM, Choung HK, Kim M, Oh S, Kim SH. Change of β-zone parapapillary atrophy during axial elongation: Boramae myopia cohort study report 3. *Investig Ophthalmol Vis Sci*. 2018;59:4020–4030.
23. Lee KM, Kim M, Oh S, Kim SH. Position of central retinal vascular trunk and preferential location of glaucomatous damage in myopic normal-tension glaucoma. *Ophthalmol Glaucoma*. 2018;1:32–43.
24. Lee KM, Choung HK, Kim M, Oh S, Kim SH. Positional change of optic nerve head vasculature during axial elongation as evidence of lamina cribrosa shifting: Boramae Myopia Cohort Study Report 2. *Ophthalmology*. 2018;125:1224–1233.
25. Coudrillier B, Boote C, Quigley HA, Nguyen TD. Scleral anisotropy and its effects on the mechanical response of the optic nerve head. *Biomech Model Mechanobiol*. 2012;12:941–963.
26. Faridi OS, Park SC, Kabadi R, et al. Effect of focal lamina cribrosa defect on glaucomatous visual field progression. *Ophthalmology*. 2014;121:1524–1530.

Investigative Ophthalmology & Visual Science

27. Park SC, Hsu AT, Su D, et al. Factors associated with focal lamina cribrosa defects in glaucoma. *Invest Ophthalmol Vis Sci*. 2013;54:8401–8407.
28. Kim YK, Jeoung JW, Park KH. Effect of focal lamina cribrosa defect on disc hemorrhage area in glaucoma. *Investig Ophthalmol Vis Sci*. 2016;57:899–907.
29. Zhang C, Tatham AJ, Medeiros FA, Zangwill LM, Yang Z, Weinreb RN. Assessment of choroidal thickness in healthy and glaucomatous eyes using swept source optical coherence tomography. *PLoS One*. 2014;9: e0109683.
30. Park HYL, Lee NY, Shin HY, Park CK. Analysis of macular and peripapillary choroidal thickness in glaucoma patients by enhanced depth imaging optical coherence tomography. *J Glaucoma*. 2014;23:225–231.
31. Maul EA, Friedman DS, Chang DS, et al. Choroidal thickness measured by spectral domain optical coherence tomography: Factors affecting thickness in glaucoma patients. *Ophthalmology*. 2011;118:1571–1579.
32. Barteselli G, Chhablani J, El-Emam S, et al. Choroidal volume variations with age, axial length, and sex in healthy subjects: A three-dimensional analysis. *Ophthalmology*. 2012;119:2572–2578.
33. Sawada Y, Araie M, Ishikawa M, Yoshitomi T. Multiple temporal lamina cribrosa defects in myopic eyes with glaucoma and their association with visual field defects. *Ophthalmology*. 2017;124:1600–1611.
34. Kimura Y, Akagi T, Hangai M, et al. Lamina cribrosa defects and optic disc morphology in primary open angle glaucoma with high myopia. *PLoS One*. 2014;9:1–18.

Investigative Ophthalmology & Visual Science